Applied Mathematics & Information Sciences
An International Journal

http://dx.doi.org/10.18576/amis/200619

Generalized Thermoelastic Response of Functionally Graded Materials Subjected to a Pulsed Heat Flux

Ibrahim Abbas[1,*], *Eman Al-Lehaibi*[2] *and Aatef Hobiny*[3]

[1]Mathematics Department, Faculty of Science, Sohag University, Sohag, Egypt
[2]Mathematics Department, Jamoum University College, Umm Al-Qura University, Jamoum 25375, Saudi Arabia
[3]Department of Mathematics, Faculty of Science, King Abdulaziz University, Jeddah, Saudi Arabia

Received: 15 Feb. 2026, Revised: 22 Mar. 2026, Accepted: 18 Apr. 2026
Published online: 1 Nov. 2026

Abstract: This study investigates generalized thermoelastic behavior in functionally graded materials (FGMs) subjected to pulsed heat flux. FGMs are characterized by material properties that vary continuously across their spatial domain. The basic equations are formulated within the framework of generalized thermoelasticity incorporating a single relaxation time and subsequently transformed into the Laplace domain. An analytical solution is derived in the transformed domain using the eigenvalue approach, while numerical inversion of the Laplace transform is employed to recover the corresponding physical-domain responses. The results are presented graphically to assess the effects of material non-homogeneity and pulse heat flux duration on the distributions of displacement, temperature, and stress.

Keywords: Laplace transform method; eigenvalue-based analytical solution; functionally graded material systems (FGMs).

Nomenclature

Symbol	Description
λ, μ	Lamé's constants
T	Temperature
t_p	Heat flux pulse time
α_t	Thermal expansion coefficient
k	Thermal conductivity
u_i	Components of displacement
ρ	Density of material
Q_o	Constant heating flux
T_o	Initial temperature
σ_{ij}	Components of stress
c_e	Specific heat
τ_o	Relaxation time
δ_{ij}	Kronecker symbol

1 Introduction

Functionally graded materials (FGMs) have received a great deal of research attention as modern composite systems featuring continuously varying composition and structure, which provide enhanced thermomechanical performance relative to conventional homogeneous materials [1]. The interaction between thermal and mechanical fields in such heterogeneous media is governed by thermoelasticity. Biot [2] established the coupled thermoelastic formulation to describe interactions between deformation and temperature fields. To overcome the unphysical implication of infinite thermal propagation speed inherent in parabolic formulations, Lord and Shulman [3] developed generalized thermoelasticity by introducing a thermal relaxation time into the heat conduction equation.

Thermal conductivity plays an essential role in regulating heat transfer within functional structures. Consequently, numerous investigations have examined temperature-dependent thermal conductivity in thermal and thermoelastic analyses. Singh et al. [4] investigated convective-radiative fins with temperature-dependent thermal properties. Pan et al. [5] experimentally verified the identification of temperature-dependent thermal conductivity. Wang et al. [6, 7] analyzed generalized solutions for axisymmetric thermoelastic problems and thick hollow cylinders with temperature-dependent properties. Xiong

* Corresponding author e-mail: ibrabbas7@science.sohag.edu.eg

© 2026 NSP
Natural Sciences Publishing Cor.

et al. [8] investigated the influence of variable thermal conductivity on generalized thermoelastic responses in fiber-reinforced half-spaces. Abbas et al. [9] explored photothermal interactions in semiconductors containing cylindrical cavities with variable conductivity.

A substantial body of research has explored wave propagation and thermomechanical behavior in functionally graded structures under various thermal and mechanical loading conditions. Das and Kanoria [10] and Mallik and Kanoria [11] investigated thermoelastic responses in functionally graded unbounded media subjected to periodically varying heat sources. Abbas and Zenkour [12] analyzed electro-magneto-thermoelastic interactions in infinite functionally graded cylinders. Othman and Abbas [13] studied thermal-shock problems in non-homogeneous hollow cylinders with energy dissipation. Abbas [14] employed the finite element method to examine magneto-thermoelastic responses in non-homogeneous cylinders.

Related investigations have also considered the thermomechanical behavior of functionally graded cylinders and plates [15], as well as thermal stresses in functionally graded beams [16]. Sur and Kanoria [17] investigated thermoelastic interactions in functionally graded viscoelastic planes. Mechanical and thermal stresses induced in two-dimensional functionally graded piezoelectric materials during steady state were discussed by Meshkini et al. [18], while magneto-thermoelastic interactions in micropolar functionally graded media were analyzed by Kalkal et al. [19]. Wang and Mai [20] solved transient heat-conduction problems using finite element formulations, whereas exact solutions were derived for steady-state thermoelastic responses in orthotropic shells by Pelletier and Vel [21]. The study of thermoelastic behavior in FGMs considering the combined effects of rotation and magnetic fields was carried out by Gunghas et al. [22].

Further developments have expanded generalized thermoelastic modeling in FGMs. Kumar et al. [23] investigated transient disturbances in nonlocal functionally graded solids under the Green–Lindsay framework. Incorporating gravitational and rotational effects, Sheokand et al. [24] analyzed thermoelastic coupling under a dual-phase-lag heat-conduction model. Boora et al. [25] studied thermomechanical interactions in rotating orthotropic FGMs under gravity. Barak and Dhankhar [26] examined the influence of inclined loading on functionally graded fiber-reinforced media. Sheoran et al. [27] explored thermodynamic interactions in rotating functionally graded semiconductor materials. In addition, Purkait and Kanoria [28] examined thermoelastic interactions using refined three-phase-lag formulations associated with the Green–Naghdi framework. A substantial body of further research [29] has addressed related problems using various generalized thermoelastic theories, highlighting the continuing development of analytical and computational approaches in this field.

2 Basic Equations

The governing equations describing generalized thermoelastic behavior in FG materials, in the absence of body forces, are formulated according to the theoretical framework presented in [3, 30] as follows:

$$\left(kT_{,i}\right)_{,i} = \left(1+\tau_o\frac{\partial}{\partial t}\right)\left(\rho c_e\frac{\partial T}{\partial t}+\gamma T_o\frac{\partial u_{i,i}}{\partial t}\right), \tag{1}$$

$$\sigma_{ij,j} = \rho\frac{\partial^2 u_i}{\partial t^2}, \tag{2}$$

$$\sigma_{ij} = \left(\lambda u_{k,k}-\gamma(T-T_o)\right)\delta_{ij}+\mu\left(u_{i,j}+u_{j,i}\right), \tag{3}$$

where $i = 1,2,3$ and $\gamma = (2\mu+3\lambda)\alpha_t$.

Accordingly, the relevant quantities λ, μ, γ, k and ρ are replaced by $\lambda_o f(X), \mu_o f(X), \gamma_o f(X), k_o f(X)$ and $\rho_o f(X)$, where $f(X)$ denotes a prescribed dimensionless function of the spatial coordinates, $X = (x,y,z)$, and $\mu_o, \lambda_o, \gamma_o, k_o$ and ρ_o represent constant parameters. Applying these substitutions to Eqs. (1)–(3) yields the following formulation:

$$\left(k_o f(X)T_{,j}\right)_{,j} = \left(1+\tau_o\frac{\partial}{\partial t}\right)\left(\rho_o c_e f(X)\frac{\partial T}{\partial t} +\gamma_o T_o f(X)\frac{\partial u_{j,j}}{\partial t}\right), \tag{4}$$

$$\begin{aligned} &f(X)\left[\mu_o\left(u_{j,i}+u_{i,j}\right)+\left(\lambda_o u_{k,k}-\gamma_o\left(T-T_o\right)\right)\delta_{ij}\right]_{,j} \\ &+f(X)_{,j}\left[\left(\lambda_o u_{k,k}-\gamma_o\left(T-T_o\right)\right)\delta_{ij}+\mu_o\left(u_{i,j}+u_{j,i}\right)\right] \\ &=\rho_o f(X)\frac{\partial^2 u_i}{\partial t^2}, \end{aligned} \tag{5}$$

$$\sigma_{ij} = f(X)\left[\mu_o\left(u_{j,i}+u_{i,j}\right)+\left(\lambda_o u_{k,k}-\gamma_o\left(T-T_o\right)\right)\delta_{ij}\right]. \tag{6}$$

The present investigation considers an isotropic functionally graded thermoelastic medium occupying the region $0 \le x \le a$, with the x-axis oriented normal to the bounding plane and directed into the medium. Assuming that all field variables depend exclusively on the spatial coordinate x and time t, the displacement vector $\mathbf{u}$ and temperature field T can be represented as:

$$\mathbf{u} = (u(x,t),0,0), \quad T = T(x,t). \tag{7}$$

Assuming that the material properties vary exclusively along the x-direction, the spatially dependent function $f(X)$ simplifies to $f(x)$. Accordingly, the governing equations within the generalized thermoelastic model with a single thermal relaxation time are formulated as follows:

$$\begin{aligned} &k_o f(x)\frac{\partial^2 T}{\partial x^2}+k_o\frac{\partial f(x)}{\partial x}\frac{\partial T}{\partial x} \\ &=\left(1+\tau_o\frac{\partial}{\partial t}\right)\left(\rho_o c_e f(x)\frac{\partial T}{\partial t}+\gamma_o T_o f(x)\frac{\partial^2 u}{\partial t\partial x}\right), \end{aligned} \tag{8}$$

© 2026 NSP
Natural Sciences Publishing Cor.

$$f(x)\left[(\lambda_o+2\mu_o)\frac{\partial^2 u}{\partial x^2}-\gamma_o\frac{\partial T}{\partial x}\right] + \frac{\partial f(x)}{\partial x}\left[(\lambda_o+2\mu_o)\frac{\partial u}{\partial x}-\gamma_o(T-T_o)\right]=\rho_o f(x)\frac{\partial^2 u}{\partial t^2}, \tag{9}$$

$$\sigma_{xx}=f(x)\left[(\lambda_o+2\mu_o)\frac{\partial u}{\partial x}-\gamma_o(T-T_o)\right]. \tag{10}$$

3 Exponential Gradation of Material Non-homogeneity

To characterize the spatial variation in material properties, an exponential distribution is adopted, defined by $f(x)=e^{nx}$, where n denotes a dimensionless parameter [11]. Substituting this expression into Eqs. (8)–(10) yields the following simplified governing equations:

$$k_o\frac{\partial^2 T}{\partial x^2}+k_o n\frac{\partial T}{\partial x}=\left(1+\tau_o\frac{\partial}{\partial t}\right)\left(\rho_o c_e\frac{\partial T}{\partial t}+\gamma_o T_o\frac{\partial^2 u}{\partial t\partial x}\right), \tag{11}$$

$$\left[(\lambda_o+2\mu_o)\frac{\partial^2 u}{\partial x^2}-\gamma_o\frac{\partial T}{\partial x}\right] + n\left[(\lambda_o+2\mu_o)\frac{\partial u}{\partial x}-\gamma_o(T-T_o)\right]=\rho_o\frac{\partial^2 u}{\partial t^2}, \tag{12}$$

$$\sigma_{xx}=e^{nx}\left[(\lambda_o+2\mu_o)\frac{\partial u}{\partial x}-\gamma_o(T-T_o)\right]. \tag{13}$$

4 Initial and Boundary Conditions

The initial conditions are assumed to be homogeneous:

$$\begin{aligned} u(x,0)&=0, \quad \left.\frac{\partial u(x,t)}{\partial t}\right|_{t=0}=0,\\ T(x,0)&=0, \quad \left.\frac{\partial T(x,t)}{\partial t}\right|_{t=0}=0. \end{aligned} \tag{14}$$

The boundary conditions are given as:

$$\begin{aligned} &\sigma_{xx}(0,t)=0, \quad \left.k(x)\frac{\partial T(x,t)}{\partial x}\right|_{x=0}=-q_o\frac{t^2 e^{-\frac{t}{t_p}}}{16t_p^2},\\ &\sigma_{xx}(a,t)=0, \quad T(a,t)=0. \end{aligned} \tag{15}$$

To recast the governing formulation into non-dimensional form, the following dimensionless variables and parameters are introduced:

$$\begin{aligned} (x',u')&=\eta_o c(x,u), \quad T'=\frac{T-T_o}{T_o},\\ (t',\tau_o')&=\eta_o c^2(t,\tau_o), \quad \sigma_{xx}'=\frac{\sigma_{xx}}{\lambda_o+2\mu_o},\\ c^2&=\frac{\lambda_o+2\mu_o}{\rho_o}, \quad \eta_o=\frac{\rho_o c_e}{k_o}. \end{aligned} \tag{16}$$

Upon omitting the prime notation from the dimensionless variables, the governing system can be expressed as:

$$\frac{\partial^2 T}{\partial x^2}+n\frac{\partial T}{\partial x}=\left(1+\tau_o\frac{\partial}{\partial t}\right)\left(\frac{\partial T}{\partial t}+g\frac{\partial^2 u}{\partial t\partial x}\right), \tag{17}$$

$$\frac{\partial^2 u}{\partial x^2}-m\frac{\partial T}{\partial x}+n\left(\frac{\partial u}{\partial x}-mT\right)=\frac{\partial^2 u}{\partial t^2}, \tag{18}$$

$$\sigma_{xx}=e^{nx}\left(\frac{\partial u}{\partial x}-mT\right), \tag{19}$$

$$\begin{aligned} u(x,0)&=0, \quad \left.\frac{\partial u(x,t)}{\partial t}\right|_{t=0}=0,\\ T(x,0)&=0, \quad \left.\frac{\partial T(x,t)}{\partial t}\right|_{t=0}=0, \end{aligned} \tag{20}$$

$$\begin{aligned} &\sigma_{xx}(0,t)=0, \quad \left.\frac{\partial T(x,t)}{\partial x}\right|_{x=0}=-q_o\frac{t^2 e^{-\frac{t}{t_p}}}{16t_p^2}e^{-nx},\\ &\sigma_{xx}(a,t)=0, \quad T(a,t)=0, \end{aligned} \tag{21}$$

where

$$m=\frac{T_o\gamma_o}{\lambda_o+2\mu_o}, \quad g=\frac{\gamma_o}{\eta_o k_o}, \quad \gamma_o=(3\lambda_o+2\mu_o)\alpha_t.$$

Applying the Laplace transform with respect to time to Eqs. (17)–(21), while incorporating the initial conditions, yields the following system of differential equations in the Laplace domain:

$$\frac{d^2\overline{u}}{dx^2}=s^2\overline{u}+nm\overline{T}-n\frac{d\overline{u}}{dx}+m\frac{d\overline{T}}{dx}, \tag{22}$$

$$\frac{d^2\overline{T}}{dx^2}+n\frac{d\overline{T}}{dx}=(s+s^2\tau_o)\left(\overline{T}+g\frac{d\overline{u}}{dx}\right), \tag{23}$$

$$\overline{\sigma}_{xx}=e^{nx}\left(\frac{d\overline{u}}{dx}-m\overline{T}\right), \tag{24}$$

$$\begin{aligned} &\overline{\sigma}_{xx}(0,s)=0, \quad \frac{d\overline{T}(0,s)}{dx}=-\frac{q_o t_p e^{-nx}}{8(st_p+1)^3},\\ &\overline{\sigma}_{xx}(a,s)=0, \quad \overline{T}(a,s)=0. \end{aligned} \tag{25}$$

Combining Eqs. (22) and (23), the governing relations can be consolidated into the following vector–matrix differential equation:

$$\frac{dV}{dx}=AV, \tag{26}$$

where

$$V=\begin{bmatrix}\overline{u}\\ \overline{T}\\ \frac{d\overline{u}}{dx}\\ \frac{d\overline{T}}{dx}\end{bmatrix}, \quad A=\begin{bmatrix}0 & 0 & 1 & 0\\ 0 & 0 & 0 & 1\\ s^2 & nm & -n & m\\ 0 & s(1+s\tau_o) & s(1+s\tau_o)g & -n\end{bmatrix}.$$

Following the eigenvalue-based approach [31, 32], the characteristic equation associated with matrix A is formulated as follows:

$$\omega^4-s_1\omega^3-s_2\omega^2+s_3\omega+s_4=0, \tag{27}$$

© 2026 NSP
Natural Sciences Publishing Cor.

where

$$
\begin{aligned}
s_1 &= -2n,\\
s_2 &= s^2 + s(1+s\tau_o) + ms(1+s\tau_o)g - n^2,\\
s_3 &= -ns(1+s\tau_o) - nm(1+s\tau_o)g - ns^2,\\
s_4 &= s^3(1+s\tau_o).
\end{aligned}
$$

The characteristic equation yields four eigenvalues $\omega_1, \omega_2, \omega_3, \omega_4$ of matrix A. The corresponding solution of Eq. (26) is expressed as:

$$V(x,s) = \sum_{i=1}^{4} A_i X_i e^{\omega_i x}, \tag{28}$$

where X_i are the eigenvectors and A_1, A_2, A_3, A_4 are arbitrary constants determined by the boundary conditions.

The time-dependent distributions of displacement, temperature, and stress are evaluated numerically using the Riemann-sum approximation for the inverse Laplace transform:

$$
\begin{aligned}
V(x,t) = \frac{e^{pt}}{t}\Bigg(&\frac{1}{2}\mathrm{Re}\left[\overline{V}(x,p)\right]\\
&+\mathrm{Re}\sum_{j=1}^{N}(-1)^j \overline{V}\left(x, p+\frac{ij\pi}{t}\right)\Bigg).
\end{aligned}
\tag{29}
$$

Here, i denotes the imaginary unit, and Re represents the real part. The choice $p = 4.7/t$ provides rapid numerical convergence [33].

5 Numerical Results

This study examines the thermoelastic behavior of an isotropic functionally graded medium subjected to laser heating with a finite-duration pulse, within the framework of generalized thermoelasticity. The material properties adopted in the numerical analysis are specified in accordance with [34] as follows:

$$
\begin{aligned}
&\lambda_o = 7.76\times10^{10}\,\mathrm{N\cdot m^{-2}}, \quad \mu_o = 3.86\times10^{10}\,\mathrm{N\cdot m^{-2}},\\
&\rho_o = 8.954\times10^{3}\,\mathrm{kg\cdot m^{-3}}, \quad T_o = 293\,\mathrm{K}, \quad t = 0.2,\\
&k_o = 3.86\times10^{2}\,\mathrm{W\cdot m^{-1}\cdot K^{-1}},\\
&c_e = 3.8310\times10^{2}\,\mathrm{J\cdot kg^{-1}\cdot K^{-1}},\\
&\alpha_t = 17.8\times10^{-6}\,\mathrm{K^{-1}}, \quad \tau_o = 0.05, \quad t_p = 0.15.
\end{aligned}
$$

The spatial variations in displacement, temperature, and stress are evaluated numerically. Figures 1–6 illustrate the resulting distributions of the physical field variables along the spatial coordinate x.

5.1 Effect of Material Non-homogeneity on Field Distributions

Figure 1 illustrates the variation in the dimensionless temperature T along the spatial coordinate x for different values of the non-homogeneity parameter n. The temperature decreases monotonically with increasing distance from the heated boundary and approaches zero as x increases. At any fixed position, the temperature decreases as n increases from 0 to 3. The homogeneous case ($n = 0$) exhibits the highest temperature, whereas the case with $n = 3$ yields the lowest temperature throughout the domain.

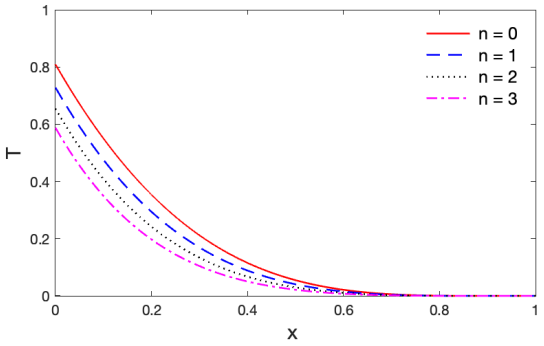


Fig. 1: Temperature distribution as a function of x for different degrees of material non-homogeneity n.

Figure 2 illustrates the variation of displacement u along the spatial coordinate x for different values of the material non-homogeneity parameter n. All curves exhibit a similar qualitative trend: the displacement initially takes negative values, increases rapidly, crosses zero, and reaches a positive maximum before gradually decaying toward zero as x increases. Increasing n from 0 to 3 reduces the magnitude of the initial negative displacement and lowers the positive peak.

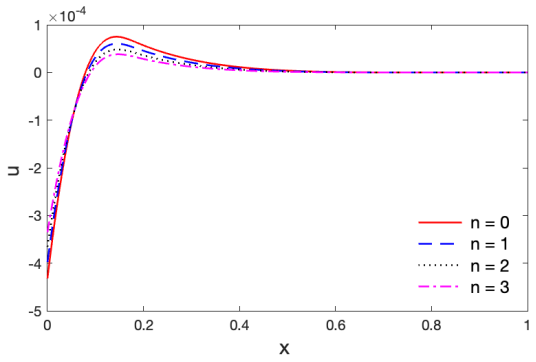


Fig. 2: Displacement distribution as a function of x for different degrees of material non-homogeneity n.

Figure 3 illustrates the variation of the normal stress component σ_{xx} along the normalized spatial coordinate x for different degrees of material non-homogeneity ($n = 0, 1, 2, 3$). The stress initially decreases from zero, reaches

© 2026 NSP
Natural Sciences Publishing Cor.

a minimum negative value (maximum compressive stress), and then gradually increases toward zero as x increases. As the degree of material non-homogeneity increases, the magnitude of the compressive stress decreases slightly.

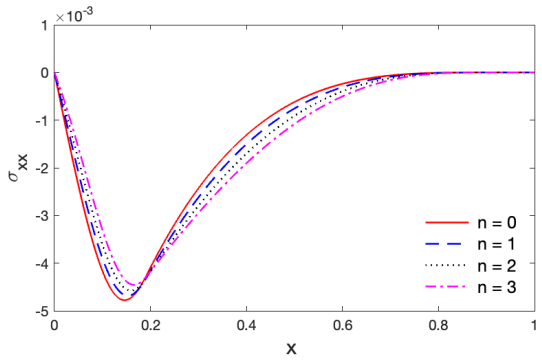


Fig. 3: Stress distribution as a function of x for different degrees of material non-homogeneity n.

5.2 Effect of Laser Pulse Duration on Field Distributions

Figure 4 presents the temperature distribution T as a function of x for different laser pulse durations t_p. The temperature decreases continuously with increasing distance from the heated surface, eventually approaching zero. For a given spatial position, shorter laser pulses produce higher temperatures, whereas longer pulse durations result in lower temperature values. Specifically, the temperature is highest for $t_p = 0.10$ and lowest for $t_p = 0.25$.

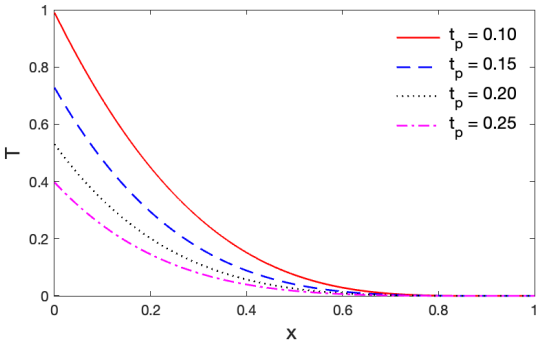


Fig. 4: Comparison of temperature distributions for different laser pulse durations t_p.

Figure 5 presents the displacement distribution for different laser pulse durations t_p. As t_p increases from 0.10 to 0.25, the initial negative displacement decreases substantially in magnitude, while the positive peak also becomes lower, indicating a weaker peak mechanical response for longer pulses under the specified model conditions.

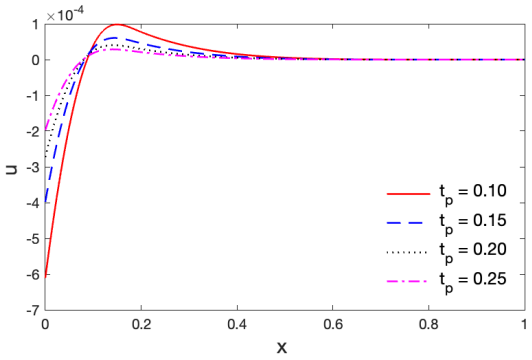


Fig. 5: Comparison of displacement distributions for different laser pulse durations t_p.

Figure 6 presents a comparison of the normal stress component σ_{xx} along the normalized spatial coordinate x for different laser pulse durations t_p. The magnitude of the compressive stress decreases significantly with increasing laser pulse duration. Shorter laser pulses generate higher compressive stress concentrations, whereas longer pulses produce a less pronounced stress response distributed over a wider spatial region.

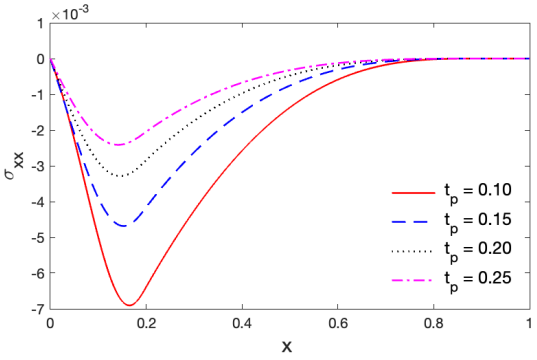


Fig. 6: Comparison of stress distributions for different laser pulse durations t_p.

6 Conclusion

This study investigated the generalized thermoelastic response of functionally graded materials subjected to pulsed heat flux. Using the Laplace transform and eigenvalue approach, analytical solutions in the transform domain were obtained and numerically inverted. The key conclusions are:

- Increasing the material non-homogeneity parameter n leads to a notable reduction in the temperature, displacement, and stress peaks throughout the medium.
- Shorter laser pulse durations induce significantly higher peak temperatures and larger compressive stress concentrations near the boundary.
- The eigenvalue approach coupled with numerical Laplace inversion provides a powerful, highly accurate analytical-numerical tool for analyzing transient

© 2026 NSP
Natural Sciences Publishing Cor.

thermomechanical responses in functionally graded solids.

Funding: This research work was funded by Umm Al-Qura University, Saudi Arabia under grant number: 26UQU4380170GSSR02.

Acknowledgment: The authors extend their appreciation to Umm Al-Qura University, Saudi Arabia for funding this research work through grant number: 26UQU4380170GSSR02.

References

[1] Delfosse, D., Fundamentals of Functionally Graded Materials— S. Suresh and A. Mortensen IOM Communications Ltd, 1998 ISBN: 1-86125-063-0. 1998, Elsevier.

[2] Biot, M.A., Thermoelasticity and Irreversible Thermodynamics. Journal of Applied Physics, 1956. 27(3): p. 240-253.

[3] Lord, H.W. and Y. Shulman, A generalized dynamical theory of thermoelasticity. Journal of the Mechanics and Physics of Solids, 1967. 15(5): p. 299-309.

[4] Singh, S., D. Kumar, and K.N. Rai, Convective-radiative fin with temperature dependent thermal conductivity, heat transfer coefficient and wavelength dependent surface emissivity. Propulsion and Power Research, 2014. 3(4): p. 207-221.

[5] Pan, W., et al., Identification of temperature-dependent thermal conductivity and experimental verification. Measurement Science and Technology, 2016. 27(7): p. 075005.

[6] Wang, Y.Z., et al., Generalized solution of the thermoelastic problem for the axisymmetric structure with temperature-dependent properties. European Journal of Mechanics - A/Solids, 2019. 76: p. 346-354.

[7] Wang, Y.Z., et al., Thermoelastic interaction in functionally graded thick hollow cylinder with temperature-dependent properties. Journal of Thermal Stresses, 2018. 41(4): p. 399-417.

[8] Xiong, C.-B., L.-N. Yu, and Y.-B. Niu, Effect of Variable Thermal Conductivity on the Generalized Thermoelasticity Problems in a Fiber-Reinforced Anisotropic Half-Space. Advances in Materials Science and Engineering, 2019. 2019: p. 1-9.

[9] Abbas, I., A. Hobiny, and M. Marin, Photo-thermal interactions in a semi-conductor material with cylindrical cavities and variable thermal conductivity. Journal of Taibah University for Science, 2020. 14(1): p. 1369-1376.

[10] Das, P. and M. Kanoria, Magneto-thermoelastic Response in a Functionally Graded Isotropic Unbounded Medium Under a Periodically Varying Heat Source. International Journal of Thermophysics, 2009. 30(6): p. 2098-2121.

[11] Mallik, S.H. and M. Kanoria, Generalized thermoelastic functionally graded solid with a periodically varying heat source. International Journal of Solids and Structures, 2007. 44(22): p. 7633-7645.

[12] Abbas, I.A. and A.M. Zenkour, LS model on electro–magneto–thermoelastic response of an infinite functionally graded cylinder. Composite Structures, 2013. 96: p. 89-96.

[13] Othman, M.I.A. and I.A. Abbas, Generalized Thermoelasticity of Thermal-Shock Problem in a Non-homogeneous Isotropic Hollow Cylinder with Energy Dissipation. International Journal of Thermophysics, 2012. 33(5): p. 913-923.

[14] Abbas, I.A., Generalized magneto-thermoelasticity in a non-homogeneous isotropic hollow cylinder using the finite element method. Archive of Applied Mechanics, 2009. 79(1): p. 41-50.

[15] Reddy, J.N. and C.D. Chin, Thermomechanical Analysis of Functionally Graded Cylinders and Plates. Journal of Thermal Stresses, 1998. 21(6): p. 593-626.

[16] Sankar, B.V. and J.T. Tzeng, Thermal stresses in functionally graded beams. AIAA journal, 2002. 40(6): p. 1228-1232.

[17] Sur, A. and M. Kanoria, Thermoelastic interaction in a viscoelastic functionally graded half-space under three-phase-lag model. European Journal of Computational Mechanics, 2014. 23(5-6): p. 179-198.

[18] Meshkini, M., et al., Steady-state thermal and mechanical stresses in Two-Dimensional Functionally Graded Piezoelectric Materials (2D-FGPMs) for a hollow infinite cylinder. Scientia Iranica, 2019. 26(1): p. 428-444.

[19] Kumar Kalkal, K., A. Gunghas, and S. Deswal, Two-dimensional magneto-thermoelastic interactions in a micropolar functionally graded solid. Mechanics Based Design of Structures and Machines, 2020. 48(3): p. 348-369.

[20] Wang, B.-L. and Y.-W. Mai, Transient one-dimensional heat conduction problems solved by finite element. International Journal of Mechanical Sciences, 2005. 47(2): p. 303-317.

[21] Pelletier, J.L. and S.S. Vel, An exact solution for the steady-state thermoelastic response of functionally graded orthotropic cylindrical shells. International Journal of Solids and Structures, 2006. 43(5): p. 1131-1158.

[22] Gunghas, A., et al., Influence of Rotation and Magnetic Fields on a Functionally Graded Thermoelastic Solid Subjected to a Mechanical Load. Journal of Mathematics, 2019. 2019(1): p. 1016981.

[23] Kumar, R., et al., Transient disturbances in a nonlocal functionally graded thermoelastic solid under Green–Lindsay model. International Journal of Numerical Methods for Heat & Fluid Flow, 2020. 31(7): p. 2288-2307.

[24] Sheokand, S.K., K.K. Kalkal, and S. Deswal, Thermoelastic interactions in a functionally graded material with gravity and rotation under dual-phase-lag heat conduction. Mechanics Based Design of Structures and Machines, 2023. 51(6): p. 3026-3045.

[25] Boora, K., S. Deswal, and A. Kadian, Thermo-mechanical interactions in a functionally graded orthotropic thermoelastic medium with rotation and gravity. Mechanics Based Design of Structures and Machines, 2024. 52(7): p. 4312-4336.

[26] Barak, M.S. and P. Dhankhar, Effect of inclined load on a functionally graded fiber-reinforced thermoelastic medium with temperature-dependent properties. Acta Mechanica, 2022. 233(9): p. 3645-3662.

[27] Sheoran, D., et al., Thermodynamical interactions in a rotating functionally graded semiconductor material with gravity. Multidiscipline Modeling in Materials and Structures, 2023. 19(2): p. 226-252.

[28] Purkait, P. and M. Kanoria, Thermoelastic Interaction in a Functionally Graded Medium Due to Refined Three-Phase-

© 2026 NSP
Natural Sciences Publishing Cor.

Lag Green–Naghdi Model under Gravitational Field. Journal of Multiscale Modelling, 2024. 14(04): p. 2350012.
[29] I. A. Abbas and A. M. Zenkour, Dual-phase-lag model on thermoelastic interactions in functionally graded media, *Journal of Thermal Stresses*, **37**, 913–923, 2014.
[30] Abbas, I.A., A problem on functional graded material under fractional order theory of thermoelasticity. Theoretical and Applied Fracture Mechanics, 2014. 74: p. 18-22.
[31] Hobiny, A., I. Abbas, and M. Marin, The Influences of the Hyperbolic Two-Temperatures Theory on Waves Propagation in a Semiconductor Material Containing Spherical Cavity. Mathematics, 2022. 10(1).
[32] Abbas, I.A., Generalized thermoelastic interaction in functional graded material with fractional order three-phase lag heat transfer. Journal of Central South University, 2015. 22(5): p. 1606-1613.
[33] Tzou, D.Y., Macro-to micro-scale heat transfer: the lagging behavior. 1996: CRC Press.
[34] Abbas, I., Generalized magneto-thermoelasticity in a non-homogeneous isotropic hollow cylinder using the finite element method. Archive of Applied Mechanics, 2009. 79(1): p. 41-50.

© 2026 NSP
Natural Sciences Publishing Cor.